

## Semiconductor electrodes. 32. n- and p-gallium arsenide n- and p-silicon, and n-titanium dioxide in liquid ammonia

Richard E. Malpas, Kingo Itaya, and Allen J. Bard

*J. Am. Chem. Soc.*, **1981**, 103 (7), 1622-1627 • DOI: 10.1021/ja00397a003 • Publication Date (Web): 01 May 2002

Downloaded from <http://pubs.acs.org> on February 13, 2009

### More About This Article

---

The permalink <http://dx.doi.org/10.1021/ja00397a003> provides access to:

- Links to articles and content related to this article
- Copyright permission to reproduce figures and/or text from this article

methanol molecule is not determined by this experiment. The distance to the OH proton is quite compatible with the present values for solvated electrons found in ethanol. We originally<sup>24</sup> suggested that the solvated electron in methanol would have an OH bond orientation, but we are now inclined to the view that it would have a molecular dipole orientation. A clear-cut resolution to this problem awaits new experimental approaches.

In summary, a general outline of the electron solvation geometry in both polar and nonpolar solvents is beginning to emerge. To some extent the current theory based on semicontinuum model potentials can semiquantitatively account for the experimental geometries for solvated electrons in ethanol and in methyltetrahydrofuran solvents, that is, for the case of large, polar solvating molecules and large, nonhydroxylic, less polar solvating molecules.<sup>18</sup> For example, the electron-to-molecular-point-dipole

distance for the first solvation shell in ethanol calculated on the basis of the semicontinuum model is 0.24 nm. One would presumably locate the point dipole near the oxygen in ethanol, so this theoretical distance correlates with the experimental distance range of 0.25–0.28 nm for the electron-to-oxygen distance determined here. However, for small, polar solvating molecules, as exemplified by water, the semicontinuum potential theoretical model, even in its ab initio incarnation,<sup>25</sup> does not satisfactorily explain the experimental geometry found.

**Acknowledgment.** This work was supported by the U.S. Department of Energy under Contract EY-76-S-02-2086. We thank P. Corfield for assistance with Figure 8.

(25) M. Newton, *J. Phys. Chem.*, **79**, 2795 (1975).

## Semiconductor Electrodes. 32. n- and p-GaAs, n- and p-Si, and n-TiO<sub>2</sub> in Liquid Ammonia

Richard E. Malpas, Kingo Itaya, and Allen J. Bard\*

Contribution from the Department of Chemistry, The University of Texas at Austin, Austin, Texas 78712. Received June 9, 1980

**Abstract:** The behavior of several n- and p-type semiconductors in liquid ammonia with 0.1 M KI as supporting electrolyte was investigated. The flat-band potentials were estimated from Schottky–Mott plots, and the current–potential curves with several redox couples (e.g., benzophenone, naphthalene, nitrobenzene) in the dark and under illumination were obtained. Photoinjection of solvated electrons at p-GaAs and p-Si was demonstrated, and the results with these materials were shown to be consistent with those from the Fermi level pinning model. Solvated electron photovoltaic cells with these semiconductors were also constructed.

### Introduction

The behavior of semiconductor electrodes in nonaqueous solvents such as acetonitrile (MeCN) is often very different than that observed in aqueous solutions.<sup>1–6</sup> The smaller interaction of the solvent with the electrode material and its oxidation products frequently results in higher stability of the semiconductor under irradiation, which is important in the design of photoelectrochemical (PEC) cells. Moreover, the wide potential range over which the solvent is stable allows the investigation of redox processes not observable in aqueous systems. There have been a number of electrochemical studies at metal electrodes in liquid ammonia.<sup>7,8</sup> Because the background limit of NH<sub>3</sub> is very negative and NH<sub>3</sub> has a low acidity, highly reduced species (e.g., radical anions, dianions) and solvated electrons are stable in this medium. In a recent study from this laboratory on the photoelectrochemical properties of p-GaAs in NH<sub>3</sub>,<sup>9</sup> we demonstrated that the photoinjection of solvated electrons at potentials ~0.9 V positive of the reversible potential for solvated electron production at a Pt electrode [–2.74 V vs. Ag/Ag<sup>+</sup> (0.1 M)<sup>8,10</sup>] could be accomplished. Such photoinjection suggested either that the conduction band edge of GaAs was situated at very negative

Table I. Semiconductor Materials

semi-conductor	source	contact	etchant
n-GaAs	Monsanto	In/Au <sup>a</sup>	(1) 3/1/1 mixture of H <sub>2</sub> SO <sub>4</sub> /H <sub>2</sub> O/30% H <sub>2</sub> O <sub>2</sub> for 5 s (2) 6 M HCl for 25 s
p-GaAs	Atomergic	Au	as n-GaAs
n-Si	Monsanto	In/Ga	5/3/3 as mixture of HNO <sub>3</sub> /HF/CH <sub>3</sub> CO <sub>2</sub> H for 10 s
p-Si	Monsanto	Au	as n-Si
n-TiO <sub>2</sub>	Fuji Titanium	In/Ga	5/3/3 mixture of HNO <sub>3</sub> /HF/CH <sub>3</sub> CO <sub>2</sub> H + 1 drop Br <sub>2</sub> per 100 cm <sup>3</sup> for 15 s

<sup>a</sup> Heated in H<sub>2</sub> to 400 °C for 2 h.

potentials compared to the location found in other solvents or that the photopotential originated from specific surface effects.

Recently, however, results from our group with p-GaAs<sup>2,11</sup> as well as by Wrighton and co-workers for p-Si<sup>12</sup> have led to our proposing that with these materials in aqueous and MeCN solutions, Fermi level pinning<sup>13</sup> occurs. This refers to the condition when the surface state density is sufficiently high that the accumulation of surface charge causes a shift in the location of the band edges; i.e., changes in the potential drop across the Helmholtz layer. More recent experiments have also suggested Fermi level

(1) Frank, S. N.; Bard, A. J. *J. Am. Chem. Soc.* **1975**, *97*, 747.

(2) Kohl, P. A.; Bard, A. J. *J. Electrochem. Soc.* **1979**, *126*, 59.

(3) Legg, K. D.; Ellis, A. B.; Bolts, J. M.; Wrighton, M. S. *Proc. Natl. Acad. Sci. U.S.A.* **1977**, *74*, 4116.

(4) Yeh, L.-S. R.; Hackerman, N. *J. Phys. Chem.* **1978**, *82*, 2719.

(5) Nakatani, K.; Tsubomura, H. *Bull. Chem. Soc. Jpn.* **1977**, *50*, 783.

(6) Frank, S. N.; Laser, D.; Hardee, K. L.; Bard, A. J. *Proc. Electrochem. Soc.* **1977**, *77-3*, p 149.

(7) Smith, W. H.; Bard, A. J. *J. Am. Chem. Soc.* **1975**, *97*, 5203, and references therein.

(8) Teherani, T.; Itaya, K.; Bard, A. J. *Nouv. J. Chim.* **1978**, *2*, 481.

(9) Malpas, R. E.; Itaya, K.; Bard, A. J. *J. Am. Chem. Soc.* **1979**, *101*, 2535.

(10) Bard, A. J.; Itaya, K.; Malpas, R. E.; Teherani, T. *J. Phys. Chem.* **1980**, *84*, 1262.

(11) Fan, F.-R. F.; Bard, A. J. *J. Am. Chem. Soc.* **1980**, *102*, 3677.

(12) Bocarsly, A. B.; Bookbinder, D. C.; Dominey, R. N.; Lewis, N. S.; Wrighton, M. S. *J. Am. Chem. Soc.* **1980**, *102*, 3683.

(13) Bard, A. J.; Bocarsly, A. B.; Fan, F.-R. F.; Walton, E. G.; Wrighton, M. S. *J. Am. Chem. Soc.* **1980**, *102*, 3671.

pinning occurs with CdTe<sup>14</sup> and molybdenum and tungsten dichalcogenides.<sup>15,16</sup> Thus the photoinjection of electrons can be explained by the pinning of the Fermi level in the p-GaAs at a level near that of  $e_s^-$ .

We report here studies of n- and p-type GaAs and Si and n-TiO<sub>2</sub> in liquid NH<sub>3</sub>. Flat-band potentials ( $V_{fb}$ ) estimated from capacitance measurements (Schottky–Mott plots) are reported, and the behavior of several organic redox couples at these materials in the dark and under irradiation is described. The key points in the work described here include (a) demonstration of solvated electron injection from p-Si at considerable underpotentials, (b) construction of a regenerative (photovoltaic) PEC in which p-Si shows stable operation, and (c) reinterpretation of the p-GaAs results in terms of the Fermi level pinning model. The results are of significance because solvated electrons represent the most reducing species thus far photogenerated at a semiconductor electrode. Their photoproduction raises a number of interesting synthetic possibilities for using light to promote reductions previously requiring alkali metals. The PEC cells with liquid NH<sub>3</sub> represent the lowest temperature PEC devices reported thus far. Several brief reports on the determination of  $V_{fb}$  for n- and p-type GaP,<sup>17</sup> the behavior of cyclooctatetrenyl dianion at n-TiO<sub>2</sub>,<sup>18</sup> and electron injection processes from several semiconductors into liquid ammonia<sup>19</sup> have appeared recently.

### Experimental Section

The single-crystal semiconductors were provided with ohmic contacts (Table I) and mounted in glass tubes as described previously.<sup>1,2</sup> The electrodes were polished with alumina and etched prior to use (Table I). The ammonia (Matheson Gas 99.9%) was purified by double distillation from sodium metal,<sup>8</sup> and 0.1 M potassium iodide was used throughout as supporting electrolyte.

The two-compartment electrochemical cell was the same as that used previously,<sup>9</sup> with a coiled Pt wire counter electrode, a silver wire reference electrode, and Pt disk and the semiconductor working electrodes. All potentials are reported vs. the Ag/AgNO<sub>3</sub> (0.1 M) reference electrode. The cell was cooled in an 2-propanol/CO<sub>2</sub> bath to approximately -50 °C.

Electrochemical measurements were carried out with a PAR 173 potentiostat, a PAR 175 Universal programmer (Princeton Applied Research Corp.), and  $i$ - $V$  curves recorded on a Houston 2000 X-Y recorder (Houston Instruments, Austin, TX). The light source was a 275-W G.E. sunlamp, which provide a total (polychromatic) intensity of ~80 mW cm<sup>-2</sup> at the electrode.

Capacitance measurements were carried out in two ways. In method a a 5-mV sinusoidal signal (Wavetek VCG 114) was superimposed on the applied dc electrode potential and the output signals from the current and voltage followers of the potentiostat were amplified and resolved into their in-phase and quadrature components (PAR 5204 lock-in amplifier). The capacitance and resistance were computed as series circuit elements. In method b the charging currents of cyclic voltammograms were measured in a region where no faradaic reaction occurs, and the capacitance was calculated from these.<sup>2</sup>

### Results and Discussion

**Capacitance Measurements.** The flat-band potential in background electrolyte solution,  $V_{fb}^0$ , which represents the potential at which no space-charge region exists within the semiconductor is often estimated by Schottky–Mott (S–M) plots.<sup>20</sup> These are plotted according to eq 1, where  $C_{sc}$  is the capacitance of the

$$\frac{1}{C_{sc}^2} = \left( \frac{2}{e\epsilon\epsilon_0 N} \right) \left( V - V_{fb}^0 - \frac{kT}{e} \right) \quad (1)$$

(14) Aruchamy, A.; Wrighton, M. S., private communication (submitted for publication).

(15) Fan, F.-R. F.; White, H. S.; Wheeler, B.; Bard, A. J. *J. Am. Chem. Soc.* **1980**, *102*, 5142.

(16) Schneemeyer, L. F.; Wrighton, M. S., private communication (submitted for publication).

(17) Belloni, J.; Amerongen, G. V.; Heindl, R.; Herlem, M.; Sculfort, J.-L. *Hebd. Seances C.R. Acad. Sci., Ser. B.* **1979**, *288*, 295.

(18) Fox, M. A.; Kabir-ud-Din J. *Phys. Chem.* **1979**, *83*, 1800.

(19) Krohn, C. E.; Thompson, J. C. *Chem. Phys. Lett.* **1979**, *65*, 132.

(20) For example, Laflere, W. H.; Van Meirhaeghe, R. L.; Cardon, F.; Gomes, W. P. *Surf. Sci.* **1976**, *59*, 401, and references therein.

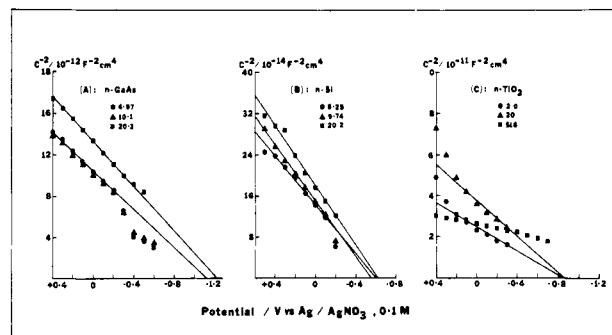


**Figure 1.** Schottky–Mott plots for n-GaAs, n-Si, and n-TiO<sub>2</sub> in NH<sub>3</sub> containing 0.1 M KI. For n-GaAs and n-Si measurement was by method a in the experimental section and the frequencies shown are in kilohertz. For n-TiO<sub>2</sub>, frequencies are in hertz. The low-frequency (2 and 20 Hz) measurements were by cyclic voltammetry whereas the measurement at 516 Hz was by method a.

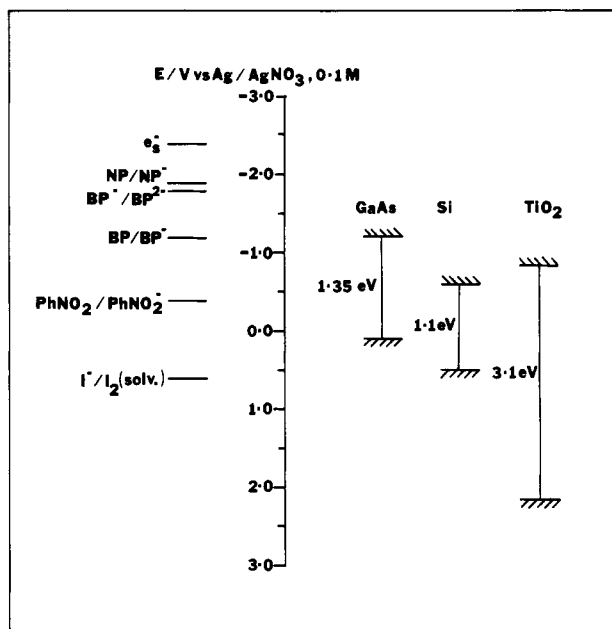


**Figure 2.** Relative position of the valence and conduction bands based on the results of S–M plots in the absence of redox couples. The reversible potentials of redox couples at a Pt electrode are also shown (NP = naphthalene; BP = benzophenone; PhNO<sub>2</sub> = nitrobenzene).

space-charge region at potentials,  $V$ , where a depletion layer is formed,  $\epsilon$  is the dielectric constant of the semiconductor, and  $N$  is the dopant density. A plot of  $1/C_{sc}^2$  vs.  $V$  for potentials positive of  $V_{fb}^0$  (for n-type materials) should be linear and intersect the potential axis near  $V_{fb}^0$ . In many cases, however, the existence of surface states, a voltage dependent  $\epsilon$ , or other factors leads to nonlinear S–M plots or plots in which the apparent  $C_{sc}$  value depends on frequency,<sup>20</sup> so that the  $V_{fb}^0$  so determined can often only be considered as approximate. S–M plots for n-GaAs, n-Si, and n-TiO<sub>2</sub> are shown in Figure 1. For n-GaAs and n-Si good linearity was obtained over a potential range of ~0.7 V, although some dependence of the  $C_{sc}$  values on frequency was noted. The results shown here (parts A and B of Figure 1) were obtained from ac measurements (method a in Experimental Section) and gave the same value of  $V_{fb}$  as that obtained from cyclic voltammetry (method b) at lower frequencies (2–20 Hz). A large frequency dispersion as well as nonlinearity was observed in the plots for n-TiO<sub>2</sub>. The plots obtained from cyclic voltammetric measurements (method b at low frequency (2 and 20 Hz) (Figure 1C)) indicate a value of  $V_{fb}$  of around -0.8 V. Plots for TiO<sub>2</sub> obtained by method a at higher frequencies (516 Hz), however, gave a much more negative value of  $V_{fb}$ . Voltammetric studies, discussed later, suggest that the former value is more accurate. The relative positions of the valence and conduction bands for these semi-

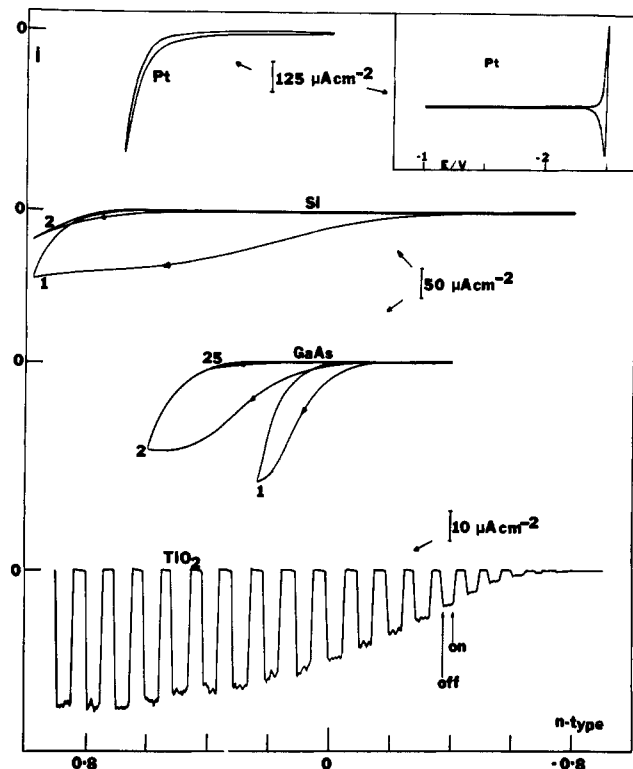


**Figure 3.** Background cyclic voltammograms for illuminated n-type semiconductors in 0.1 M KI solution. The inset is the background cyclic voltammogram on a Pt disk electrode (scan rate = 200 mV/s): 1, first scan; 2, second scan, immediately following 1.

conductors in a supporting electrolyte solution of 0.1 M KI, based on the S-M plots, are shown in Figure 2. Because of the frequency dispersion effects discussed above, the values of  $V_{fb}^0$  are probably only accurate to  $\pm 0.2$  V.

**Voltammetric Studies.** Cyclic voltammetry (CV) at the semiconductor electrodes was carried out in the dark and under illumination in the absence and in the presence of a number of compounds that undergo reversible one-electron charge-transfer processes at Pt. Typically the couples utilized were benzophenone (BP), naphthalene (NP), and nitrobenzene ( $\text{PhNO}_2$ ), whose behavior at metal electrodes in liquid  $\text{NH}_3$  has been previously investigated.<sup>7</sup> The reversible potentials of these are indicated in Figure 2. The most negative potential for the onset of anodic photocurrent for an n-type semiconductor and the most positive potential for the onset of cathodic photocurrent for a p-type semiconductor ( $V_{on}$ ) are often used in the estimation of the position of  $V_{fb}^0$  where  $V_{fb}^0$  is the flat-band potential found in the absence of a redox couple. Care must be taken in this identification, however, since surface changes or recombination processes can cause these onset potentials to differ from the true  $V_{fb}^0$  values. Moreover,  $V_{fb}$  may change upon specific adsorption of an ionic species or, as discussed below, on Fermi level pinning,<sup>13</sup> these effects may yield  $V_{on}$  values which are functions of the redox couple present in solution. The details of the voltammetric behavior of each semiconductor are discussed below.

**n-GaAs.** The background CV of n-GaAs in the dark at potentials negative of  $V_{fb}$  in 0.1 M KI was identical with that at Pt (Figure 3, inset) and showed a reversible wave beginning at  $-2.4$  V accompanied by the characteristic blue color for solvated electron ( $e_s^-$ ) generation.<sup>8,10</sup> On illumination a photoanodic current was observed at potentials positive of  $\sim -0.1$  V (Figure 3). However, repeated scans in this potential region produced a decrease in current, suggesting that changes in the electrode surface, e.g., photooxidation of the GaAs lattice, were occurring. Similar behavior has been observed previously for n-GaAs electrodes in DMF.<sup>4</sup> Species with  $V_{redox}$  values (as estimated from CV at Pt) negative of the conduction band edge ( $V_{on}$ ,  $-1.2 \pm 0.2$ ) would be expected to show essentially reversible behavior in the dark at n-type semiconductors, at potentials similar to those on Pt, due

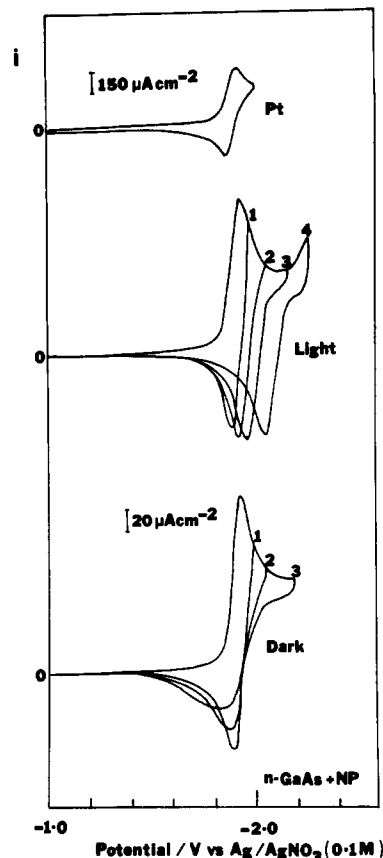


**Figure 4.** Cyclic voltammogram of naphthalene on a Pt disk electrode and on n-GaAs in the dark and on illumination (scan rate = 200 mV/s). Numbers on curves represent the scan sequence.

to the presence of an accumulation layer in the space-charge region. This behavior was observed for both  $e_s^-$  generation and for naphthalene (Figure 4). Reoxidation of  $\text{NP}^-$  on scan reversal occurred at the same potential as on Pt in the dark. However, under illumination, while the cathodic wave was unaffected, the anodic wave shifted toward slightly more positive potentials; the extent of this shift was a function of switching potential ( $V_\lambda$ ) (Figure 4). However, values of  $V_\lambda$  negative of  $\sim -2.0$  V produced anodic waves with  $V_{pa}$  values at more negative potentials than the cathodic wave.

Benzophenone (BP) forms the radical anion,  $\text{BP}^-$ , on reduction. Since the redox potential of this couple is located near  $V_{fb}$  of n-GaAs, no photoeffect is expected for the oxidation reaction. BP produced an irreversible wave for reduction commencing just negative of  $V_{fb}^0$  in the dark and resulting in a broad peak with  $V_{pc}$  at  $\sim -1.9$  V (Figure 5). However, illumination with chopped light gave a photooxidation peak with  $V_{pa}$  at  $-1.6$  V for reoxidation of the  $\text{BP}^-$  found on the negative scan. Thus as with NP, photoeffects were observed on n-GaAs at potentials well negative of the  $V_{fb}^0$  found in supporting electrolyte solution alone.

**p-GaAs.** The behavior of p-GaAs electrodes in the dark is shown in Figure 6. The onset of anodic current occurs at  $+0.1$  V ( $\sim V_{fb}^0$  from S-M plots) and, as with the anodic photocurrent at n-GaAs, decreased with repeated scanning, again suggesting surface changes upon oxidation of the semiconductor. Under illumination photogeneration of  $e_s^-$  was observed as reported previously.<sup>9</sup>

The CV of NP on p-GaAs in the dark and on illumination is shown in Figure 7. In the dark only a small cathodic current was observed at potentials negative of  $V_{redox}$  (NP). On illumination, however, photoreduction of NP commenced at  $\sim -1.3$  V with  $V_{pc} \approx -1.6$  V. Repeated scanning to a more positive switching potential,  $V_\lambda$  (but still negative of  $\sim -0.9$  V) caused a shift in the potential for current onset and  $V_{pc}$  toward more positive potentials to a limiting value for current onset,  $V_{on}$ , of  $\sim -1.0$  V. This represents an underpotential for the photoreduction of about 0.8 V which is similar to that observed for  $e_s^-$  photogeneration. When

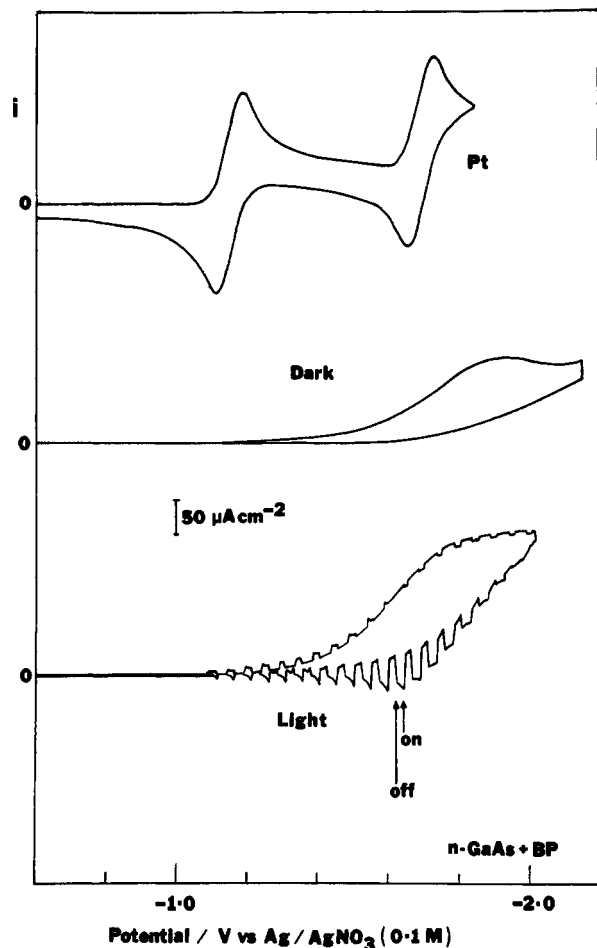


Figure 5. Cyclic voltammogram of benzophenone on a Pt disk electrode and on n-GaAs in the dark and on pulsed illumination (scan rate = 100 mV/s).

the potential was scanned to values positive of  $\sim -0.5$  V, the original CV (1 on Figure 7) was obtained on the return scan.

Benzophenone also showed photoeffects at p-GaAs electrodes. In the dark (Figure 8), only a slight increase in cathodic current was observed at  $\sim -2.0$  V. For  $V_{\lambda}$  values negative of this potential, the reverse scan produced crossing of the  $i$ - $V$  curves (i.e., hysteresis), followed by a very small anodic peak whose location and magnitude depended on  $V_{\lambda}$ . Coulometric generation of increasing amounts of  $BP^{\cdot-}$  at a Pt electrode followed by positive-going potential scans from  $-1.5$  V gave CV behavior at p-GaAs which was similar to that observed in the absence of excess  $BP^{\cdot-}$ , suggesting that the small anodic peak is due to  $BP^{\cdot-}$  oxidation produced in small amounts on the negative scans.

On pulsed illumination (Figure 8) photoreduction of benzophenone commenced at about  $-0.4$  V with  $V_{on}$  being somewhat dependent on light intensity and with a  $V_{pc}$  for the first wave of  $-0.9$  V. During the dark periods at these potentials, an anodic current was observed due to the reoxidation of photogenerated  $BP^{\cdot-}$ . Commencing at  $-1.1$  V (the onset of BP reduction on Pt), a cathodic current was observed during the dark periods following the illumination pulses. The photoreduction of  $BP^{\cdot-}$  occurred at  $\sim -1.4$  V; some dark cathodic current following the light pulses was seen beginning at  $-1.6$  V, a potential corresponding to the second BP reduction wave ( $BP^{\cdot-} + e^- \rightarrow BP^{2-}$ ) on Pt. Photogeneration of  $e_s^-$  commenced at  $\sim -1.7$  V. The current observed during the dark periods was diffusion controlled and was fairly reproducible on cycling in the dark after illumination, provided that the potential remained negative of  $\sim -0.8$  V. Cycling to 0 V gave the original dark CV.

The behavior of both n- and p-GaAs is generally consistent with the Fermi level pinning model<sup>13</sup> and with results previously found for this material in aqueous<sup>11</sup> and MeCN<sup>2</sup> solutions. Thus at p-GaAs photoreductions are observed for couples ( $e_s^-$ ,  $NP^{0/-}$ ,

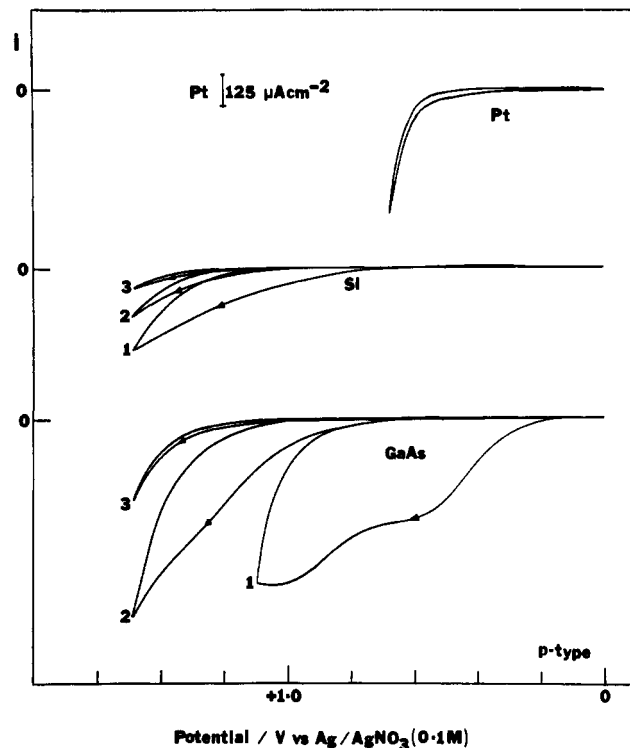


Figure 6. Background dark cyclic voltammograms for p-type semiconductors in 0.1 M KI solution (scan rate = 200 mV/s). Numbers on curves represent the scan sequence.

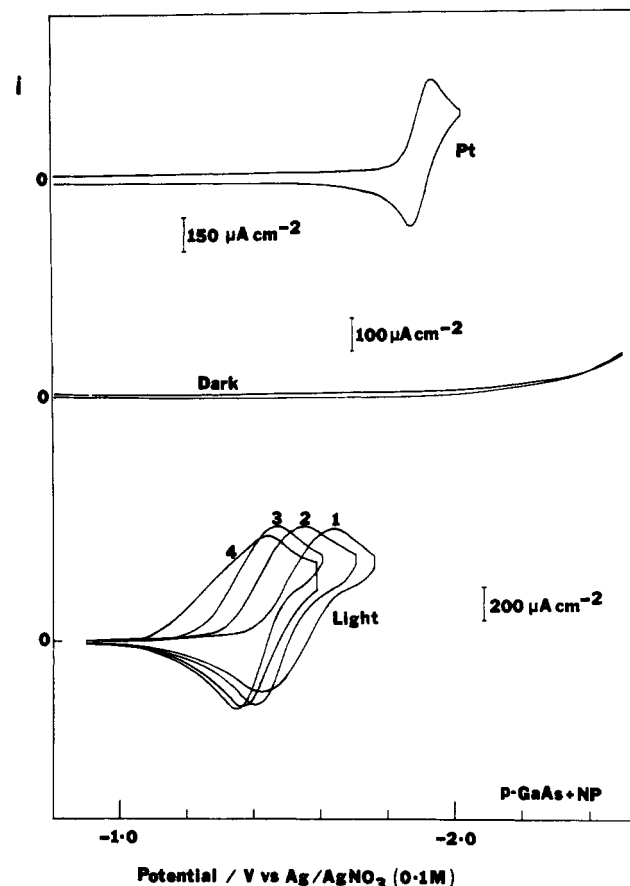


Figure 7. Cyclic voltammogram of naphthalene on a Pt disk electrode and on p-GaAs in the dark and on illumination (scan rate = 200 mV/s). Numbers on curves represent the scan sequence.

$BP^{2-}$ ) lying at potentials appreciably more negative than the conduction band edge estimated from a S-M plot in background solution. The observed value of  $V_{on} - V_{redox}$  in all of these was

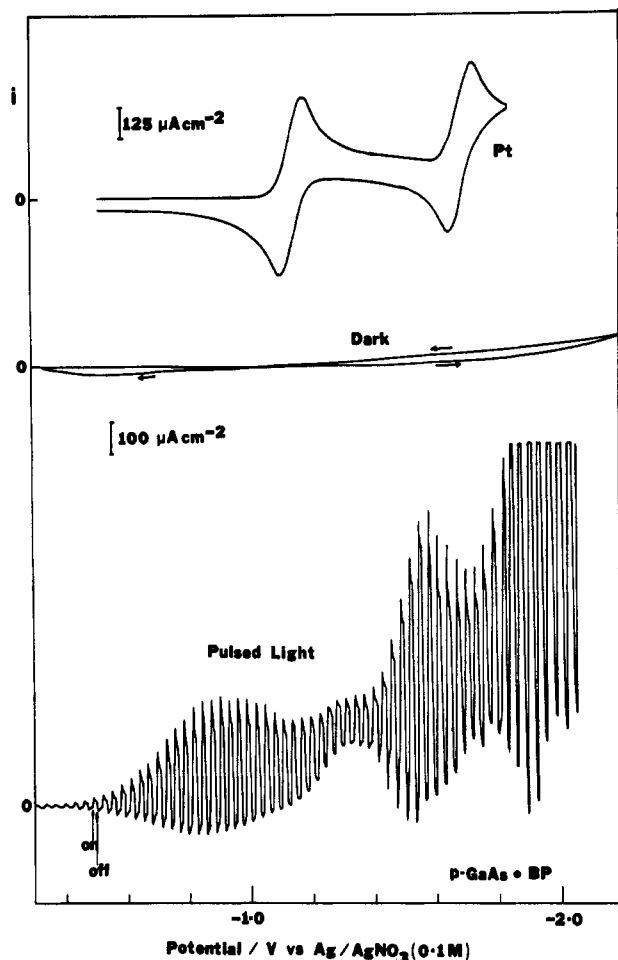
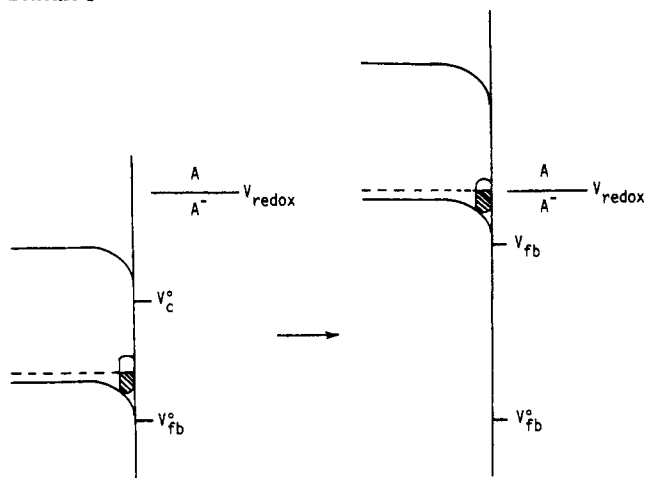


Figure 8. Cyclic voltammogram of benzophenone on a Pt disk electrode (scan rate = 200 mV/s) and on p-GaAs in the dark and under pulsed illumination (scan rate = 50 mV/s).

#### Scheme I



$\sim 0.8$  V (but somewhat dependent on the potentials to which the electrode was subjected and the light density). These results are consistent with a high density of surface states located about 0.8 eV below the conduction band edge. These states pin the semiconductor Fermi level and equilibrate with the redox couple in solution as shown in Scheme I. The shifts in  $V_{on}$  with repeated scans to different potentials (e.g., Figure 7) may represent continual shifts in  $V_{fb}$  as the charge accumulated in the surface states changes. However, such shifts could also be attributable to a chemical sense to reduction of the electrode surface by scans to negative potentials. This type of argument was originally presented in studies of the GaAs/MeCN interface<sup>2</sup> where an actual surface

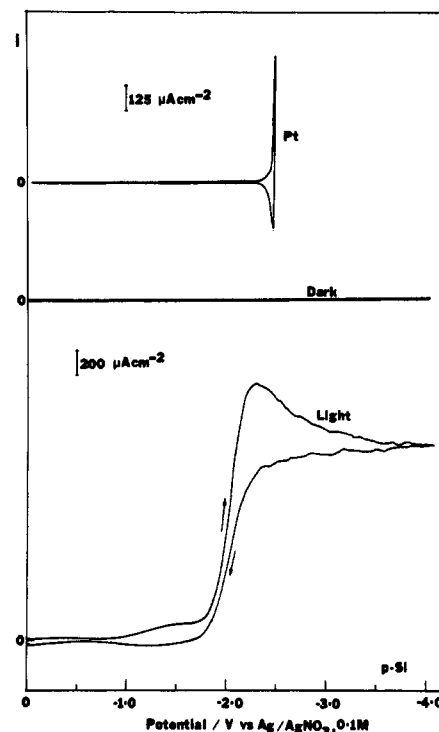


Figure 9. Background cyclic voltammograms of a Pt disk electrode and p-Si in the dark and on illumination (scan rate = 200 mV/s).

layer forming a Schottky junction with the underlying semiconductor was proposed. To probe this possibility, X-ray spectra were taken of the surface of GaAs electrodes before use and after photogeneration of solvated electrons. Peaks at 41 and 44 eV were observed in the spectrum of both electrodes, consistent with As in GaAs and arsenic oxide (possibly  $As_2O_3$ ), respectively.<sup>21</sup> The ratio of peak heights, however, changed significantly between electrodes, suggesting a thinner surface oxide film on the electrode at the potential of solvated electron photogeneration. The removal of oxide films from anodized GaAs, by etching with HCl or aqueous  $NH_3$  solutions, has previously been shown to yield a surface rich in elemental As,<sup>21</sup> a semimetal or semiconductor of band gap 1.1 eV.<sup>22</sup> The Ga peaks in the XPS spectra of the two GaAs samples were also examined, but there was very little difference between the two electrodes. Clearly the chemical or molecular nature of the surface states and the effect of surface pretreatment of the semiconductor on its photoelectrochemical behavior are of importance.<sup>23</sup> Further studies on this system to elucidate these effects are contemplated.

**n- and p-Si.** The dark negative background CV for n-Si was identical with that on Pt. On illumination a photoanodic current was observed at  $\sim -0.4$  V (Figure 3) just positive of  $V_{fb}^0$  from S-M plots as expected. The current decrease found on consecutive scans probably indicates a change in the nature of the electrode surface. The dark anodic background behavior of p-Si is shown in Figure 6. An anodic reaction commenced at +0.6 V in agreement with the value of  $V_{fb}^0$  from S-M plots. The negative background behavior is shown in Figure 9. In the dark, no current was observed even at potentials as negative as -4.0 V. On illumination, however, the photogeneration of  $e_s^-$  occurred at  $\sim -1.8$  V (the small prewave shown in Figure 9 was caused by impurities and was not always seen for p-Si/ $NH_3$  systems). The photocurrent was directly proportional to light intensity with the decrease in current at potentials negative of -2.6 V being due to absorption of the light by  $e_s^-$  generated near the electrode surface; similar effects were

(21) Chang, C. C.; Citrin, P. H.; Schwartz, B. J. *Vac. Sci. Technol.* **1977**, *14*, 943.

(22) Kelley, M. J.; Bullett, D. W. *Solid State Commun.* **1976**, *18*, 593.

(23) Bard, A. J.; Fan, F.-R. F.; Gioda, A. S.; Nagasubramanian, G.; White, H. S. *Discuss. Faraday Soc.*, in press.

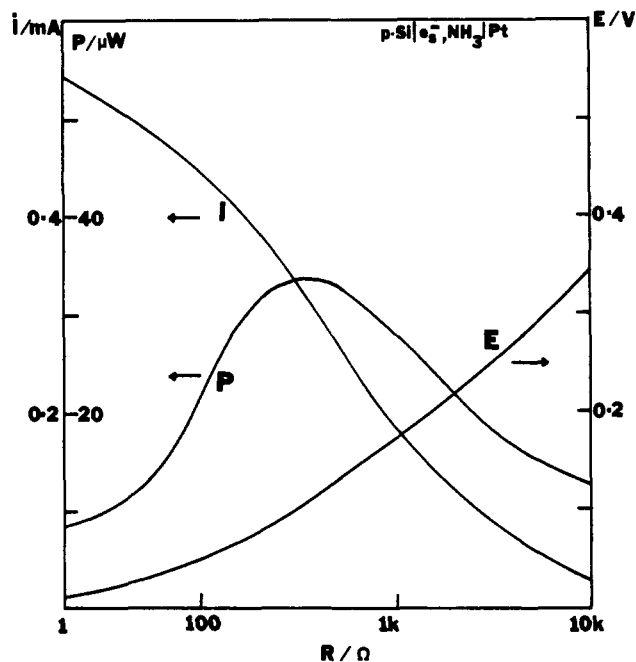


Figure 10. Current, voltage, and power curves for the photoelectrochemical cell p-Si/ $e_s^-$  (0.3 mM), 0.1 M KI, in  $\text{NH}_3$ /Pt under illumination of  $\sim 80 \text{ mW cm}^{-2}$ .

seen with  $e_s^-$  generation at p-GaAs.<sup>9</sup>

A PEC photovoltaic cell was formed, as for p-GaAs, consisting of a p-Si photocathode and Pt anode in a solution containing  $e_s^-$  (0.3 mM) generated coulometrically. An open-circuit potential,  $V_\infty$  for this cell of +570 mV, was measured on a Keithley 600A electrometer (input resistance  $10^{14} \Omega$ ) when the cell was illuminated with the sunlamp. The current, voltage, and power curves for different values of load resistance are shown in Figure 10.  $V_\infty$  was independent of the  $e_s^-$  concentration and remained constant over a period of approximately 2 h. No attempts were made to optimize the performance of this PEC cell or study its long-term behavior. However, the ability to generate a photocurrent  $\sim 0.6 \text{ mA}$  in a cell disconnected from any power sources clearly demonstrates the photoinjection of  $e_s^-$  from p-Si into  $\text{NH}_3$  (with the collection of  $e_s^-$  at the Pt counter electrode). This cell, like the p-GaAs cell previously described<sup>9</sup> represents a rather unique electrochemical system where light "pumps" electrons through the solution as well as through the external circuit. Note that Krohn and Thompson<sup>19</sup> have also reported the injection of  $e_s^-$  from p-Si into  $\text{NH}_3$ .

Benzophenone was also photoreduced on p-Si commencing at  $\sim -1.0 \text{ V}$  with a plateau at  $\sim -1.8 \text{ V}$  just prior to  $e_s^-$  generation. As with  $e_s^-$  generation, no reoxidation of photogenerated  $\text{BP}^-$  was observed.

The generation of  $e_s^-$  at p-Si occurs at potentials well negative of the background solution conduction band edge of p-Si. Again a surface state Fermi level pinning model can account for this behavior. Wrighton and co-workers<sup>12</sup> previously have shown pinning at p-Si electrodes and the equilibration of surface state levels, even with the very negative level associated with  $e_s^-$  in ammonia, can account reasonably for the observed photoinjection of electrons.

**n-TiO<sub>2</sub>.** The dark background behavior of  $\text{TiO}_2$  on scanning to negative potentials again was identical with that on Pt. On

illumination a photoanodic current was observed (Figure 3) commencing at  $-0.8 \text{ V}$ , which is about the value of  $V_{fb}^0$  obtained from the low-frequency Schottky-Mott plots (Figure 1 C). The photocurrent was reproducible and light intensity dependent, suggesting that it was due to photooxidation of the supporting electrolyte ( $\Gamma^-$ ) or solvent. Species with  $V_{redox}$  values negative of  $V_{fb}^0$  (e.g., benzophenone) were reversibly reduced in the dark on  $\text{TiO}_2$  at potentials essentially the same as those on Pt, as expected for an n-type semiconductor in the absence of surface effects. Similarly  $e_s^-$  generation occurred essentially as on Pt. For species located in the band gap, e.g., nitrobenzene ( $\text{PhNO}_2$ ), irreversible dark reduction occurred at  $\sim -0.7 \text{ V}$ ; however, no photooxidation of the generated nitrobenzene radical anion ( $\text{PhNO}_2^-$ ) was observed on illumination. Moreover, in the presence of  $\text{PhNO}_2$ , the photooxidation of the background electrolyte disappeared.

The CV behavior, with the exception of the absence of the photooxidation in the presence of  $\text{PhNO}_2$ , is essentially similar to the behavior of  $\text{TiO}_2$  in MeCN.<sup>1</sup> The oxidation of the supporting electrolyte in liquid  $\text{NH}_3$  corresponds to energy levels in the band gap of  $\text{TiO}_2$  (+0.6 V). Thus the background photooxidation of the electrolyte by holes generated in the valence band is far more favorable in  $\text{NH}_3$  than in MeCN, and the oxidation of species whose redox levels fall within the band-gap region will depend upon the relative rates of reaction of such species and background electrolyte or solvent with the photogenerated holes.

In general, the behavior of n- $\text{TiO}_2$  in  $\text{NH}_3$  appears to follow the more "ideal" interface model, where  $V_{fb}$  remains essentially fixed. This is also borne out by the carbanion photooxidation experiments of Fox and Kabir-ud-Din,<sup>18</sup> whose estimate of  $V_{fb}$  was very close to the one reported here. The behavior in the presence of  $\text{PhNO}_2$  under illumination is unusual, however. We have not previously observed such a quenching of the photocurrent by a solution species. We might note that Krohn and Thompson<sup>19</sup> report no photocurrent at n- $\text{TiO}_2$  in  $\text{NH}_3$  with NaCl,  $\text{NH}_4\text{Cl}$ , or  $\text{KNH}_2$  as supporting electrolytes.

Finally, previous studies of n- $\text{TiO}_2$  in MeCN<sup>1</sup> or aqueous solutions provided evidence for surface states or an intermediate level located 1–1.2 eV below the conduction band edge. Since this corresponds to  $\sim 0.6 \text{ V}$  vs.  $\text{Ag}/\text{AgNO}_3$ , where background oxidation occurs, probing the region of more positive potentials to provide information about such levels will be difficult in  $\text{NH}_3$ .

## Conclusions

The behavior of semiconductors in liquid ammonia generally parallels that found with aprotic solvents and water. The results can be interpreted in terms of the ideal model for n- $\text{TiO}_2$  and with the Fermi level pinning model for GaAs and Si. PEC photovoltaic cells can be constructed in this solvent system, and preliminary experiments suggest stable operation of GaAs and Si (although further experiments are necessary to establish the ultimate long-term stability and performance). Perhaps the most intriguing aspect of these experiments is the ability to photogenerate solvated electrons at p-Si and p-GaAs at potentials considerably less negative than the reversible potential for this species. This represents the photoproduction of the most negative (or reducing) species so far reported at a semiconductor and raises the possibility of utilizing such photoemitted electrons for synthetic purposes, e.g., a "Photo-Birch reduction".

**Acknowledgment.** We wish to thank J. Herrmann for the XPS measurements. The financial support of the Robert A. Welch Foundation and the National Science Foundation (Grant CHE 8000682) is gratefully acknowledged.